

Flux pinning by ordered oxygen-deficient phases in nearly stoichiometric $\text{YBa}_2\text{Cu}_3\text{O}_{7-\delta}$ single crystals

João L. Vargas and David C. Larbalestier

Department of Materials Science and Engineering and Applied Superconductivity Center, University of Wisconsin-Madison, 1500 Johnson Drive, Madison, Wisconsin 53706

(Received 4 November 1991; accepted for publication 3 February 1992)

We propose that the critical currents of nearly stoichiometric $\text{YBa}_2\text{Cu}_3\text{O}_{7-\delta}$ single crystals ($\delta < 0.1$) are determined by fluxon pinning at ordered oxygen-vacancy domains. Since these domains are also superconducting, albeit with lower T_c and H_c than the stoichiometric matrix, their pinning strength at a given temperature will increase as they are driven normal by an increasing applied field. Experimentally, the magnetization hysteresis curves display a secondary maximum, characteristic of pinning by a superconducting second phase. The ordered-vacancy domains are assumed to result from a spinodal decomposition. The density and size of the domains were calculated on this assumption. The bulk pinning force was computed by direct summation. In the limit of low temperatures, the calculated values of critical current density J_c are in good agreement with measurements on high-quality single crystals.

It has been recently shown that the flux pinning of almost stoichiometric high-quality $\text{YBa}_2\text{Cu}_3\text{O}_{7-\delta}$ single crystals is directly controlled by the oxygen deficiency.¹ Pinning by oxygen defects was found to be significant even when $\delta < 0.05$. The magnetization hysteresis at fields of several tesla decreased by factors of 3–5 as the equilibrium value of δ approached zero.¹ The magnetization curves also displayed an anomalous secondary peak at high-field (referred to sometimes as a “fish-tail” or “bow-tie”). Thus any pinning model for single crystals must take into account that (i) J_c is of order 10^6 A cm⁻² at low T , (ii) J_c increases as δ increases from zero to approximately 0.1, and (iii) at a given temperature, the hysteresis goes through a minimum and then increases as B increases, peaking at high field values.

Pinning by atomic scale defects, particularly oxygen vacancies, was previously proposed.^{2,3} Recently, the elementary pinning force of single oxygen vacancies randomly distributed in the CuO_2 planes was estimated in the limit of zero field and temperature.⁴ However, neutron diffraction data showed that the oxygen vacancies are not located in the CuO_2 but in the CuO (“chain”) layers⁵ and that significant vacancy ordering in oxygen-deficient material can occur even at room temperature.^{6,7} Ordered vacancy domains were detected in oxygen-deficient material by transmission electron microscopy (TEM).^{8,9} This result was recently confirmed by neutron diffraction.¹⁰ The most commonly observed structure consists of ordered oxygen vacancies located at $(0, 1/2 b_0, 0)$ every other unit cell. This arrangement generates a superlattice with a doubled unit cell parameter in the a direction and has the $\text{YBa}_2\text{Cu}_3\text{O}_{6.5}$ composition. This orthorhombic II (OII) structure has been associated with the 50–60 K transition temperature (T_c) plateau that has been observed for δ around 0.5.^{8,9} Electron diffraction experiments demonstrated the three-dimensional coherence of the OII structure.^{8,11} A spinodal transformation from a single non-stoichiometric phase into various ordered superlattices was also predicted in theoretical work on oxygen-deficient $\text{YBa}_2\text{Cu}_3\text{O}_{7-\delta}$.^{12–14}

We propose that the anomalous magnetization hysteresis ΔM results from the flux pinning provided by a microstructure consisting of a dilute mixture of $\text{YBa}_2\text{Cu}_3\text{O}_{6.5}$ (OII) in $\text{YBa}_2\text{Cu}_3\text{O}_7$ (OI) generated by a spinodal decomposition. The pinning centers are the ordered oxygen-deficient OII regions. Here, for the sake of simplicity we restrict the model to the OII structure but other superstructure phases (e.g., $\text{O}_{6.67}$) could also be considered. Nevertheless, the important point is that these regions are also superconducting, but have lower H_{c2} and T_c than the matrix. As was shown earlier for low-temperature superconductors, superconducting pinning centers will generate peaks in ΔM when they are driven normal as B and T are increased.¹⁵ This behavior fulfills requirement (iii) stated above. In order to verify whether the model also fits requirements (i) and (ii), we must calculate the domain size and density within the restriction of the small δ values of nearly stoichiometric material. We calculated these quantities using the assumption that the average center-to-center spacing between randomly distributed domains (called the decomposition wavelength λ_d) is constant in the early stages of the spinodal transformation.¹⁶ From published electron micrographs,^{11,17} we get a very rough estimate of the average separation between domains, $\lambda_d \approx 25$ nm. Thus, for a fixed λ_d , the size of the domains is initially controlled by the oxygen-vacancy concentration δ , which is in turn controlled by the equilibration temperature (T_a).

The equilibrium density of vacancies n_v is given by $5.75 \times 10^{27} \times \delta$ [m⁻³] and the volume fraction ν_{OII} occupied by OII domains is $\nu_{\text{OII}} = 2 n_v V_{1237} = 2\delta$, where the equilibrium δ values are taken from the literature¹⁸ and $V_{1237} = 174$ (Å³) is the volume of the $\text{YBa}_2\text{Cu}_3\text{O}_7$ unit cell. For the range of temperatures typically used (450–375 °C), δ varies from 0.0371 to 0.0121 and ν_{OII} from 7.4% to 2.4%. Standard quantitative stereology equations¹⁹ are used to calculate the radius $r = 3\lambda_d \nu_{\text{OII}}/4$ [m] and the area density $n = 3\nu_{\text{OII}}/2\pi r^2$ [m⁻²], under the assumption of a random distribution of spherically shaped domains. The domain size $2r$ varies from 2.8 to 0.9 nm, and

TABLE I. Volume fraction and size of $\text{YBa}_2\text{Cu}_3\text{O}_{6.5}$ (OII) regions as a function of the equilibration temperature in 1 atm O_2 for a model microstructure consisting of spherical domains of OII randomly distributed in the $\text{YBa}_2\text{Cu}_3\text{O}_7$ (OI) matrix. The average spacing is fixed at 25 nm.

O_2 anneal T_a ($^\circ\text{C}$)	Oxygen deficiency δ	OII volume fraction v_{OII} (%)	OII size $2r$ (nm)
450	0.0371 ^a	7.4	2.8
425	0.0265 ^b	5.3	2.0
400	0.0165 ^a	3.3	1.2
375	0.0121 ^b	2.4	0.9

^aData from Ref. 18.

^bInterpolated values from data presented in Ref. 18.

n from 1.4×10^{16} to 7.2×10^{16} [m^{-2}]. The predictions of the model are summarized in Table I.

The small size of the OII regions matches the fluxon diameter very well ($2\xi_{ab} \approx 3$ nm in the low-temperature limit). The separation of the OII regions (≈ 25 nm) corresponds to the fluxon spacing at fields around 5 T. In this situation, fluxon core pinning is a likely pinning interaction. The fluxon core interaction with the ordered OII domains yields interaction energy δE given by

$$\delta E = -\frac{1}{2}\mu_0[(H_{c\text{OI}})^2 - (H_{c\text{OII}})^2]V_i \quad [J],$$

where H_c is the thermodynamic critical field and V_i the volume of the fluxon contained in the pinning center. The elementary pinning force f_p is given by $f_p = \delta E/\xi_{ab}$, where ξ_{ab} is the coherence length ξ_{ab} for $H \parallel c$.²⁰ From the model predictions shown in Table I, we conclude that $\xi_{ab} > r$, thus the interaction volume is $4/3 \pi r^3$.

An upper limit to the bulk pinning force F_p is given by the full summation of the elementary pinning interactions, i.e., $F_p = n f_p$ [N/m^3], where n is the number density of interactions. The predicted area density of OII domains exceeds the fluxon density $n_{\text{fl}} = B/\phi_0$ [m^{-2}] over the range $B < 10$ T ($n_{\text{fl}} \leq 4 \times 10^{15} \text{ m}^{-2}$) so that full summation occurs over all the fluxons, n_{fl} . Thus F_p can be calculated from

$$F_p = \frac{\pi B \mu_0 [(H_{c\text{OI}})^2 - (H_{c\text{OII}})^2] r^2 v_{\text{OII}}}{2 \phi_0 \xi_{ab}} \quad [\text{N m}^{-3}],$$

and the critical current density is calculated using $J_c = F_p/B$. Values of $H_{c\text{OI}}(0)$ (1.55 T); $H_{c\text{OII}}(0)$ (0.38 T), and $\xi_{ab}(0)$ (1.6 nm) from single-crystal measurements²¹ are used. We assume that $H_c(T)$ follows $H_c(0)(1-t^2)$ where $t = T/T_c$, and $\xi_{ab}(T)$ is calculated from $\phi(T) = \phi(0)(1-t)^{-1/2}$.

The experimental values of the critical current density were calculated from magnetization hysteresis measurements on a high quality flux-grown single crystal²² oxygenated at 420°C for 150 h. Measurements were made in the $H \parallel c$ configuration using a vibrating sample magnetometer in a 12-T superconducting magnet. The field was ramped at about 10 mT/s at constant temperature. Representative loops are shown in Fig. 1. In Fig. 2, we present the critical current densities as a function of field calculated using the standard expression $J_c = 3\Delta M/\ell$, where ℓ is the average size of the two sides of an approximately square, plate-

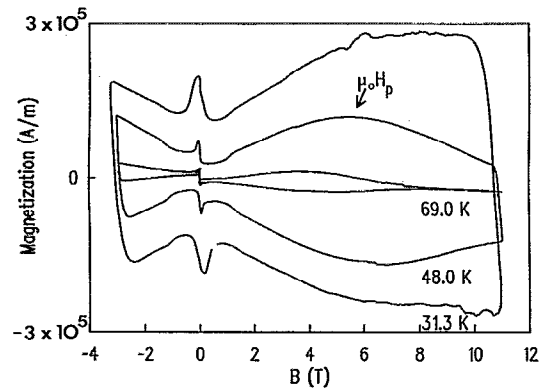


FIG. 1. Magnetization loops at several temperatures for a flux-grown single crystal annealed at 420°C in 1-atm O_2 .

shaped single crystal measuring $253 \mu\text{m} \times 225 \mu\text{m} \times 150 \mu\text{m}$ thick. Our model predictions of J_c as a function of temperature are presented in Fig. 2 together with experimental values.

The prominent feature of these curves is a peak (H_p) present at high fields. These peak-shaped magnetization curves are now well established and have been observed by several groups for a wide variety of flux grown single crystals.^{23,24} The peaks are definitely not associated with matching of fluxon and defect spacing, since the peaks move to lower fields, as the temperature is increased. These peaks are a consequence of the fact that the pinning centers are also superconducting.^{1,15} Since the pins have a lower T_c and H_{c2} than the matrix, they become normal as temperature and field are increased, therefore their pinning strength initially increases as the field is increased. When the pins are fully normal, their pinning strength is maximum. For example, the hysteresis at 48 K and 5 T is approximately four times larger than that at 1 T.

A key point is that the density of OII domains is still large (of order 10^{16} m^{-2}) even when δ is small. The model fits requirement (ii) since the pinning center size and volume fraction, which directly influence J_c , increase by a

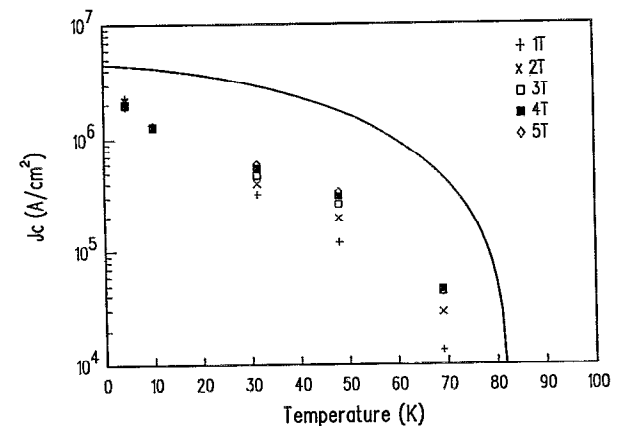


FIG. 2. Critical current density as a function of temperature. The solid line corresponds to the model for $\delta = 0.0265$ (equilibration $T_a = 425^\circ\text{C}$).

factor of 3 as the annealing temperature is varied from 375 to 450 °C, in agreement with previously published results.¹

Verification of requirement (i) by comparison to the magnitude of J_c is most trustworthy in the limits of T and H tending to zero, since flux creep, percolation, and granularity effects are then minimized.^{1,25,26} Prior work has shown that an effective granularity is observed in the same crystals that have the anomalous peak in ΔM .¹ Thus J_c tends to be underestimated, particularly for fields above the peak, since all J_c values in Fig. 2 use the full crystal dimensions for the scaling length. As T and H increase, flux creep effects become stronger, thus the experimental values of $J_c(T)$ fall off more rapidly than the model predicts. It is not clear at this stage if the granularity effect is correlated with the presence of the domains or not. For these reasons it is not easy to devise an experimental test which yields a direct comparison between predicted and experimental values over the *whole* temperature and field range.

The presence of ordered domains in off-stoichiometric material ($\delta > 0.15$) has been demonstrated⁸⁻¹⁰ but in nearly stoichiometric crystals, the domains have not been observed. However, this is expected given that the small volume fraction predicted approaches the detection limits of these techniques. Magnetization hysteresis measurements are more sensitive to oxygen-deficiency effects than microstructural techniques, although the interpretation is dependent on models such as the one presented here.

In summary, the flux pinning of flux-grown single crystals is controlled by oxygen defects and the magnetization characteristics depend on the oxygen vacancy concentration and ordering state. We have modeled the core pinning interactions between fluxons and domains of the $\text{YBa}_2\text{Cu}_3\text{O}_{6.5}$ OII phase. Even when the oxygen deficiency of single crystals is small ($\delta < 0.05$), the vacancies produce a dense distribution of domains which act as pinning centers and generate J_c values of the order 10^6 A cm^{-2} at low T .

We are grateful to D. L. Kaiser for providing the single crystals and critical reviewing of the manuscript, wish to acknowledge stimulating discussions with M. Daeumling, L. D. Cooley, G. Stejic, P. D. Jablonski, and P. Camus. This work has been supported by NSF-Materials Research Group Grant 8911332. J. L. Vargas is thankful for the

financial assistance of the C. W. Nave Fellowship.

- ¹M. Daeumling, J. M. Seuntjens, and D. C. Larbalestier, *Nature* **346**, 332 (1990).
- ²M. Tinkham, *Helv. Physica Acta* **61**, 443 (1988).
- ³D. C. Larbalestier, S. E. Babcock, X. Cai, M. Daeumling, D. P. Hampshire, T. F. Kelly, L. A. Lavanier, P. J. Lee, and J. M. Seuntjens, *Physica C* **153-155**, 1580 (1988).
- ⁴P. H. Kes, *Physica C* **185-189**, 288 (1991).
- ⁵J. D. Jorgensen, M. A. Beno, D. G. Hinks, L. Soderholm, K. J. Volin, R. L. Hitterman, J. D. Grace, and I. K. Schuller, *Phys. Rev. B* **36**, 3608 (1987).
- ⁶B. M. Veal, A. P. Paulikas, H. You, H. Shi, Y. Fang, and J. W. Downey, *Phys. Rev. B* **42**, 6305 (1990).
- ⁷K. G. Vandervoort, G. W. Crabtree, Y. Fang, S. Yang, H. Claus, and J. W. Downey, *Phys. Rev. B* **43**, 3688 (1991).
- ⁸R. J. Cava, A. W. Hewat, E. A. Hewat, B. Batlogg, M. Marezio, K. M. Rabe, J. J. Krajewski, W. F. Peck, Jr., and L. W. Rupp, Jr., *Physica C* **165**, 419 (1990).
- ⁹R. Beyers, B. T. Ahn, G. Gorman, V. Y. Lee, S. S. Parkin, M. L. Ramirez, K. P. Roche, J. E. Vasquez, T. M. Gur, and R. A. Huggins, *Nature* **340**, 619 (1990).
- ¹⁰T. Zeiske, R. Sonntag, D. Hohlwein, N. H. Andersen, and T. Wolf, *Nature* **353**, 542 (1991).
- ¹¹J. Reyes-Gasga, T. Krelkel, G. Van Tendeloo, G. Van Landuyt, S. Amelinckx, W. H. M. Bruggink, and H. Verweij, *Physica C* **159**, 831 (1989).
- ¹²A. G. Khachatryan and J. W. Morris, *Phys. Rev. Lett.* **61**, 215 (1988).
- ¹³D. de Fontaine, G. Ceder, and M. Asta, *Nature* **343**, 544 (1990).
- ¹⁴L. T. Wille, A. Berera, and D. de Fontaine, *Phys. Rev. Lett.* **60**, 1065 (1988).
- ¹⁵J. D. Livingston, *Appl. Phys. Lett.* **8**, 319 (1966).
- ¹⁶J. W. Cahn, *Trans. Met. Soc. AIME* **242**, 166 (1968).
- ¹⁷C. H. Chen, D. J. Werder, L. F. Schneemeyer, P. K. Gallagher, and J. V. Waszczak, *Phys. Rev. B* **38**, 2888 (1988).
- ¹⁸T. B. Lindemer, J. F. Hunley, J. E. Gates, A. L. Sutton, Jr., J. Brynestad, C. R. Hubbard, and P. K. Gallagher, *J. Am. Cer. Soc.* **72**, 1775 (1989).
- ¹⁹E. E. Underwood, in *Metals Handbook*, 8th ed. (American Society for Metals, Metals Park, OH, 1973), Vol. 8, pp. 37-47.
- ²⁰A. M. Campbell and J. E. Evetts, *Adv. Phys.* **21**, 199 (1972).
- ²¹K. G. Vandervoort, U. Welp, J. E. Kessler, H. Claus, G. W. Crabtree, W. K. Kwok, A. Umezawa, B. W. Veal, J. W. Downey, and A. P. Paulikas, *Phys. Rev. B* **43**, 13042 (1991).
- ²²D. L. Kaiser, F. Holzberg, B. A. Scott, and T. R. McGuire, *Appl. Phys. Lett.* **51**, 1040 (1987).
- ²³H. Küpfer, I. Apfelstedt, R. Flükiger, C. Keller, R. Meier-Hirmer, B. Runtsch, A. Turowski, U. Wiech, and T. Wolf, *Cryogenics* **29**, 268 (1989).
- ²⁴L. Civale, M. W. McElfresh, A. D. Marwick, F. Holtzberg, C. Feild, J. R. Thompson, and D. K. Christen, *Phys. Rev. B* **43**, 13732 (1991).
- ²⁵A. P. Malozemoff, *Physica C* **185-189**, 264 (1991).
- ²⁶A. Gurevich, *Phys. Rev. B* **42**, 4857 (1990).